Estimating Boat-Wake-Induced Levee Erosion using Sediment Suspension Measurements

Bernard O. Bauer[1]; Mark S. Lorang[2]; and Douglas J. Sherman[3]

Abstract: The subaqueous portion of a levee bank in the Sacramento–San Joaquin River Delta of central California was instrumented to quantify the impact of boat-generated waves. Typical erosion rates associated with recreational craft are too small for direct measurement of bank retreat on a per-boat-passage basis; therefore, two independent analytical methods of estimating linear erosion were developed based on colocated suspended sediment concentration and velocity time series. The algorithms were tested using data measured during a field experiment in which a 7.5 m boat was driven past the site over a range of speeds to generate waves of varying size. A cross-shore array of electromagnetic current meters and optical back-scatterance sensors measured the character of boat-generated waves and the resultant sediment suspension. In near-bank, shallow-water ($d<0.5$ m) locations, sediment suspension was closely correlated with the primary boat-wake waves ($H_{max}<0.21$ m), indicating that maximum near-bottom orbital velocities were sufficient to erode the fine-grained (mud-silt) bottom materials. Suspension events were short lived (order of 1–5 min), despite very long particle settling times (order of hours), because river currents swept the suspension plumes downstream. This implies negligible sedimentation and resuspension locally. Both algorithms produced strikingly similar erosion estimates, and these values (0.01–0.22 mm/boat passage) compare favorably with direct measurements of cumulative bank erosion in response to multiple, sequential boat passages. Field conditions for which the algorithms are appropriately applied are discussed.

DOI: 10.1061/(ASCE)0733-950X(2002)128:4(152)

CE Database keywords: Sediment suspension; Levees; Erosion; Ship motion; California; Measurement.

Introduction

Bank erosion along rivers, canals, and other navigable waterways is a major concern in many parts of the world. Management agencies and policy makers are intensely interested in erosion from boat-generated waves, which has been a point of contention and controversy for decades (Johnson 1958, 1968; Ofuya 1970; Collins and Noda 1971; Anderson 1974; Limerinos and Smith 1975; Camfield et al. 1980; Bhowmik and Demissie 1983; Nanson et al. 1994; Foda 1995; Osborne and Boak 1999). Most studies focusing specifically on boat-wake-induced erosion (e.g., Das and Johnson 1970) estimate erosion potential based on simple wave energy or wave power indices. Collins and Noda (1971) and Limerinos and Smith (1975) adopted such an approach for the levee banks of the Sacramento–San Joaquin River Delta in California and assumed that erosion was linearly related to energy expenditure. Conclusions about the relative importance of various fluid processes, such as channel flow, tidal currents, wind waves, and boat wakes, differ considerably. Foda (1995) argues that these differences originate in the varying methodologies and assumptions employed to estimate energy and erosion, and in the absence of direct measurements, such ambiguity is likely to persist.

To our knowledge, no field study has successfully quantified erosion rates on muddy levee banks on a per-boat-passage basis simply because few robust technologies exist with the sensitivity and precision to accurately measure such small erosion rates at reasonable cost. Thus, indirect means of estimating linear erosion associated with boat wakes must be relied upon, and these have many attendant sources of uncertainty (statistical, methodological, and natural). There exists a pressing need for development of analytical methods and for well-instrumented experiments aimed at quantifying the linkages between boat-generated waves and bank erosion. Until inexpensive technologies are developed to directly measure bank erosion of the order of tenths to hundredths of millimeters, it is imperative that the accuracy of erosion estimates be contemplated in the context of methodological uncertainty.

The goal of this study was to document, in real time and in a near-bank position, the mean currents, orbital velocities, and suspended sediment concentrations in a water column affected by recreational boat traffic. Two independent methods of estimating linear bank erosion rates on the basis of these measurements and basic sediment transport theory are derived and assessed. The results from the algorithms are compared with long-term measurements of cumulative bank retreat in response to multiple, sequential boat passages as a gauge of the accuracy of the methods.

[1]Professor, Dept. of Geography, Univ. of Southern California, Los Angeles, CA 90089-0255.

[2]Research Associate, Flathead Lake Biological Station, Univ. of Montana, Polsen, MT 59860-9659.

[3]Professor, Dept. of Geography, Texas A&M Univ., College Station, TX 77843.

Note. Discussion open until December 1, 2002. Separate discussions must be submitted for individual papers. To extend the closing date by one month, a written request must be filed with the ASCE Managing Editor. The manuscript for this paper was submitted for review and possible publication on January 23, 2001; approved on January 11, 2002. This paper is part of the ***Journal of Waterway, Port, Coastal, and Ocean Engineering***, Vol. 128, No. 4, July 1, 2002. ©ASCE, ISSN 0733-950X/2002/4-152–162/$8.00+$.50 per page.

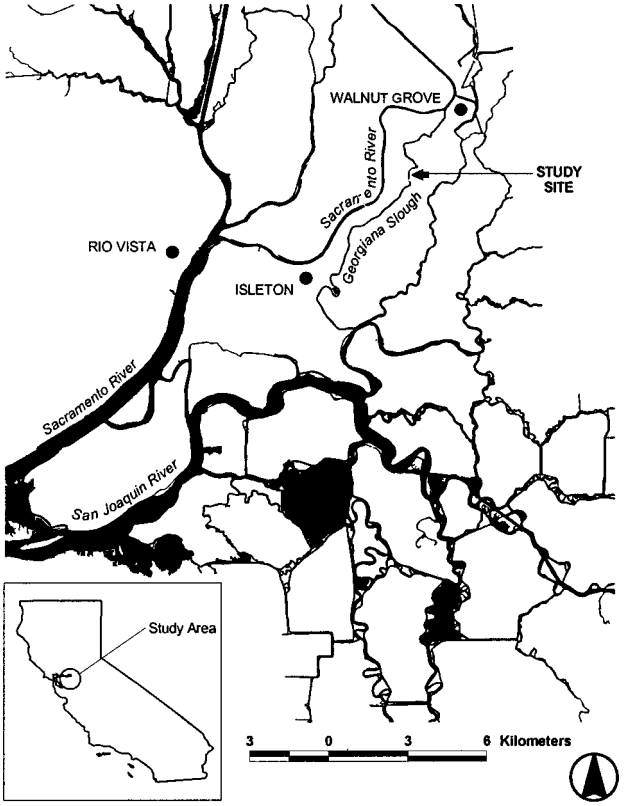

Fig. 1. Location of study site

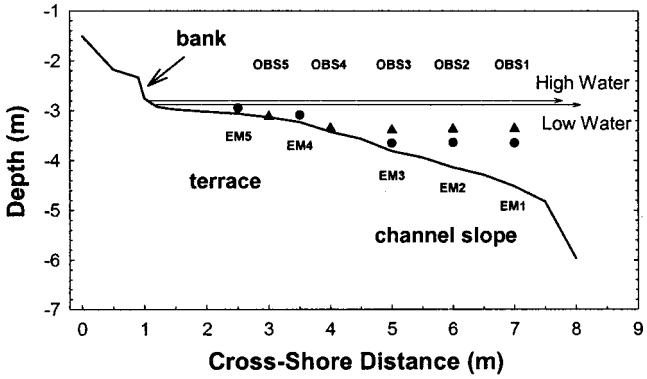

Fig. 2. Cross-sectional profile and instrument deployment scheme: Circles and triangles indicate EMs and OBSs, respectively

Research Design

Site Selection

Site selection was guided by the need to find a location that was suffering from chronic wave erosion while also displaying attributes of natural geomorphic adjustment, as indicated by (1) no armor or recent maintenance activity; (2) lack of vegetation cover; (3) presence of a vertical cut-bank; and (4) presence of a horizontal or gently sloping, subaqueous terrace. In addition, it seemed prudent to select a quasi-linear section of riverbank in order to minimize complications due to wave refraction or secondary flow effects associated with meandering reaches, bank scallops, and trees. A site in Georgiana Slough near Walnut Grove, Calif. (Fig. 1), satisfied all these criteria. Terrace and bank materials at the field site are a compacted, cohesive clay and silt mixture, and virtually all sediment transport in near-bank locations occurs in suspension. The estimated bulk density of the cohesive clay and silt mixture is approximately 2,000 kg m^{-3} (Buckman and Brady 1969). Minor lenses of fine sand can be found in the levee banks depending on the source and historic emplacement of dredge material, and even though these unconsolidated lenses may be sites of preferential bank erosion, this fine sand is an inconsequential component of the sediment transport system. The channel is approximately 40 m wide through this reach of Georgiana Slough, and even though there are strong tidal influences, this is a predominantly fluvial system (i.e., no flow reversals).

Sampling Design

Instruments were deployed in a cross-shore array (Fig. 2) that included five optical back-scatterance sensors (OBS1–OBS5) and five electromagnetic current meters (EM1–EM5). EM5 was located 1.6 m from the bank, with other instruments located sequentially farther into the channel to a distal point of 6.1 m from the bank. Sensor signals were sampled at a frequency of 0.2 Hz using a computer-based data-acquisition system. The EMs (Marsh-McBirney Model 511) are robust instruments with standard factory calibrations not prone to drift. The OBS sensors (D&A Instrument Company, Model OBS-3) were calibrated in the field through the data-acquisition system, producing linear least-squares regression fits between voltage output and suspended sediment concentrations with R^2 values of 0.99 or better.

Table 1. Summary of Boat Passage Parameters and General Hydrodynamic Conditions at EM5

		Boat parameters			Wave parameters		
Run	Time	Speed (knots)	Direction	Water depth (m)	U_d[a] (m s^{-1})	V_d[a] (m s^{-1})	Height[b] (m)
1	6:48:42	12	Downstream	0.32	0	0.04	0.18
2	7:03:34	15	Downstream	0.29	0.01	0.08	0.21
3	7:11:10	18	Upstream	0.27	0.02	0.08	0.18
4	7:22:27	6	Downstream	0.24	0.01	0.07	0.07
5	7:29:35	6	Upstream	0.22	0.01	0.06	0.06
6	7:38:41	23	Downstream	0.20	0.01	0.07	0.12
7	7:48:04	23.5	Upstream	0.18	0.01	0.07	0.12

[a]U_d, V_d refer to mean drift (river) velocity assessed from preevent segment of time series prior to boat-wake event. Positive values indicate onshore (U_d) and downstream (V_d).

[b]Wave height was calculated using linear shallow-water theory with maximum orbital velocity in onshore direction.

A 7.5 m speedboat with a sharp chine and planing hull was used to generate waves. Seven boat passages are examined in this paper (Table 1) representing three speeds (slow, medium, fast) with both upstream and downstream approaches. Each data run lasted 8–10 min, which was sufficient for all boat-generated wave activity and sediment suspension to be cleared from the channel (i.e., background conditions restored). The entire sequence of runs was completed within a 1-h period beginning with the early-morning high tide of May 20, 1997. The tide dropped 0.14 m during the experimental runs, and this change in water depth was accounted for in subsequent calculations.

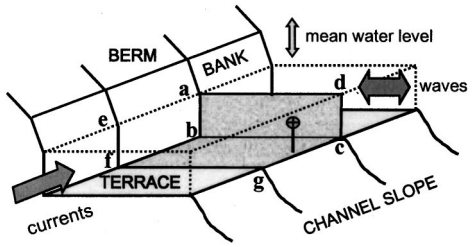

Fig. 3. Schematic of control volume and contributing area for sediment transport calculations

Analytical Methods

Colocated EM and OBS pairs facilitate the examination of phase relationship between individual waves and suspension plumes (e.g., Garrad and Hey 1987). The importance of individual waves in the wake event can be assessed directly and the magnitude of sediment transport can be estimated easily. Nevertheless, an OBS time series does not provide a direct measure of erosion rate. Linking the dynamics of sediment suspension to actual bottom erosion can be accomplished, in theory, using the erosion equation (e.g., McLean 1990) or, more generally, the sediment continuity relationship for an infinitesimally small control volume (e.g., Julien 1995; p. 176). Practically, however, these theoretical expressions are difficult to implement when the total volume of sediment in motion is relatively small and when spatial gradients in sediment concentration and flux are not pronounced (as is the case in suspension-dominated systems). Intensive instrument deployment schemes are necessary to provide sufficient spatially distributed data to accurately quantify the sediment flux divergence and flux gradient terms that characterize the advection, mixing, and diffusion components in the sediment continuity relationship. This implies high levels of financial investment, and as a consequence, less ambitious instrument deployment schemes are often used with attendant simplifications to the comprehensive theoretical equations. The analytical challenge, therefore, is to develop methods that take full advantage of time-series data from a single instrument or colocated pair of instruments to provide robust estimates of bank erosion.

Two alternative algorithms were developed in this study with the following caveats and assumptions: (1) a single bulk density value is representative of the entire terrace; (2) near-bank geometry is quasi-uniform in the along-stream direction (i.e., the terrace width is constant); (3) local OBS and EM measurements are representative of average conditions in the control volume; (4) sediment contributions from far-upstream sources (i.e., beyond the instrumented embayment) or from other erosive processes (e.g., bank collapse) are negligible for any single boat-wake event; and (5) local deposition and resuspension of sediments are negligible (i.e., eroded sediment is swept away and does not settle locally). Clearly, the long-term geomorphic evolution of levee banks is more complicated than these assumptions allow. Bank undercutting by tractive stresses and wind waves, bank material weakening and collapse due to biogeomorphic factors and dessication cycles, or direct bank-face erosion during spring floods are all known to occur over the long term. Nevertheless, these influences are outside the purview of this study, which focuses exclusively on the short-term impact of single boat passages. The last assumption in the list is critical and is justified by the observation that the settling times of fine-grained particles at our study site are of the order of tens of minutes to several hours (as indicated by the OBS calibration exercise). Near-bank river currents were of sufficient magnitude (order of 0.04–0.08 $\mathrm{m\,s^{-1}}$) to advect suspended sediments downstream for several hundreds of meters or more before particle settling could have occurred. The rapid decay evident in our suspended sediment concentration time series, therefore, implies rapid dilution by clear water from upstream rather than local particle settling.

Method 1

The basis of Method 1 is a simplified version of the erosion equation through which the time-rate-of-change in bed elevation is related to the time-rate-of-change in suspended sediment volume (McLean 1990). Horizontal sediment flux divergence terms are considered negligible (i.e., spatial gradients in sediment flux and sediment concentration are small), and the dominant suspension processes are presumed to occur only in the vertical. This does not preclude horizontal advection of sediments, but it does require that the horizontal fluxes are much greater than the spatial gradients in flux. Implementation of the method requires (1) a representative value for the volume concentration of bed material; (2) suspended sediment time series that are representative of sediment volume concentration in the entire vertical column of water above the point of interest; (3) identification of a contributing bed area from which the suspended sediments are derived; and (4) a representative (control) volume of water through which the sediments are dispersed (Fig. 3). In this study, the levee bank fixed the inner boundary of the contributing area and control volume (line segment ''ab''), whereas the outer boundary was taken to be the location of OBS5 (line segment ''cd''). Area and volume estimates were closed using water surface elevation and unit along-stream distance.

The wetted perimeter is the linear distance along the subaqueous portion of the bank and terrace from the point where the mean water level intersects the levee bank to the location of OBS5 (line segment ''abc''). Visual observations in the field suggest that, on average, sediments were stripped uniformly from this wetted perimeter during boat-wake events. It is acknowledged that such uniform stripping of sediment from the bank face and subaqueous terrace is inconsistent with long-term bank retreat, but in the absence of additional information or observations to the contrary, it is a reasonable model of how boat-generated waves erode levee banks. Falling tide reduces the length of the wetted perimeter, the size of the contributing area, as well as the volume of water above the contributing area. These changes in system attributes for each data run were factored into the calculations. The OBS time series were used to calculate the sediment mass in a water column of unit area above the contributing area ($\mathrm{g\,L^{-1}} \times 1{,}000\ \mathrm{L\,m^{-3}}$). Linear erosion rates were estimated by multiplying this sediment mass by the total control volume per unit length of channel bank ($\mathrm{m^3\,m^{-1}}$), dividing by the wetted perimeter (m), and dividing by the bulk density of in situ bottom sediments ($2 \times 10^6\ \mathrm{g\,m^{-3}}$).

Method 2

Method 2 is a novel hybrid approach. Once again, the horizontal sediment flux divergence terms are considered to be negligible, and much of the formalism inherent to the sediment continuity equation is avoided. Unlike Method 1, in which only the time-rate-of-change of suspended sediment concentration is related to erosion rate, Method 2 focuses specifically on the magnitude of sediment discharge (i.e., the product of fluid velocity and sediment concentration) and its temporal character. This quantity is commonly used in nearshore studies to assess the magnitude and direction of sediment transport under combined waves and longshore currents (e.g., Beach and Sternberg, 1988, 1991, 1992; Aagaard and Greenwood 1994; Osborne and Vincent 1996). A time-dependent estimate of erosion depth $[ED(T)]$ is calculated from

$$ED(T)=\frac{Q_{\Sigma}(T)}{CA(T)} \tag{1}$$

where $Q_{\Sigma}(T)$ = cumulative sediment volume transport (m^3) through a cross-sectional plane perpendicular to the flow (''abcd'' in Fig. 3) during elapsed time since the start of an event, T; and $CA(T)$ = contributing area from which the sediment is derived (m^2). At the start of an event, the contributing area has no size and it is equivalent to the wetted perimeter (line segment ''abc'' in Fig. 3). As time elapses, line segments ''ae,'' ''bf,'' and ''cg'' expand uniformly, presuming unidirectional flow downstream. The size of the contributing area is therefore equal to the sum of planes ''bcgf'' (i.e., the upstream terrace segment) and ''abfe'' (i.e., the upstream submerged bank segment), which is proportional to the product of flow velocity, elapsed time, and wetted perimeter as follows:

$$CA(T)=\overline{U(T)}\cdot T\cdot wp \tag{2}$$

where $\overline{U(T)}=(1/T)\int_0^T U(t)dt$ is an expanding-block-averaged velocity; $U(t)$ = instantaneous velocity perpendicular to the plane; and wp = wetted perimeter of the contributing area (constant for a given event). The product $\overline{U(T)}\cdot T$ can be interpreted as a contributing upstream length (proportional to line segments ''ae,'' ''bf,'' or ''cg''), and it is equivalent to the net streamwise distance traveled by a particle during time T prior to crossing the measurement plane. In Method 2, the contributing area is a time-dependent quantity.

Cumulative sediment volume transport is given by

$$Q_{\Sigma}(T)=\int_0^T Q_S(t)dt=\int_0^T q_S(t)\cdot A\,dt \tag{3}$$

where $Q_s(t)$ = sediment volume discharge ($m^3\,s^{-1}$); A = cross-sectional area of the plane perpendicular to the flow (m^2); and $q_s(t)$ = specific sediment flux ($m^3\,s^{-1}\,m^{-2}$). Specific sediment flux is equivalent to sediment volume discharge per unit area, and it is calculated from

$$q_S(t)=\frac{q_m(t)}{\rho_b}=\frac{C_m(t)\cdot U(t)}{\rho_b} \tag{4}$$

where $q_m(t)$ = sediment mass flux ($kg\,m^{-3}\,m\,s^{-1}$); ρ_b = bulk density of in situ bottom sediment ($kg\,m^{-3}$); and $C_m(t)$ = instantaneous sediment mass concentration ($kg\,m^{-3}$). Instantaneous sediment mass concentration is obtained directly from the calibrated OBS time series, and it is assumed that suspended sediment travels with the fluid. This is generally the case for very fine particles such as those found at the study site, but a correction factor could be easily introduced to take account of relative velocity differences (e.g., Madsen 1991).

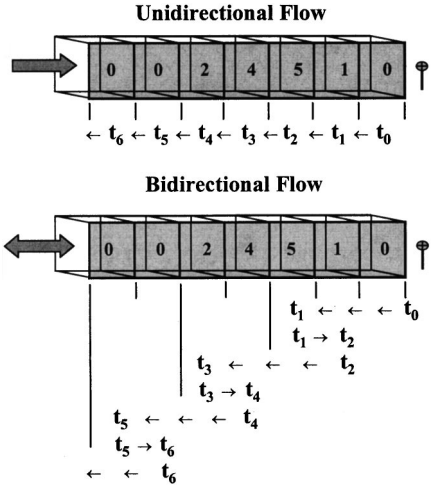

Fig. 4. Cartoon of suspended sediment boxes advected past an OBS sensor presuming simple unidirectional and bidirectional flow scenarios: arrows indicate distance steps associated with velocity increments from time t_0 through t_6; corresponding SSC and velocity time series given in Table 2 (see text for explanation).

Comparison of Methods

Fig. 4 and Table 2 demonstrate how the algorithms in Methods 1 and 2 operate to produce estimates of linear bank erosion. Presume that a single impulse wave traverses a subaqueous terrace and causes sediment to be ejected into the water column. Along-stream variation in erosion is likely, and the block distribution of sediment suspension concentration (SSC) in Fig. 4 (column 2 of Table 2) shows one possible outcome. Each block has an along-stream length of 0.1 m (with unit width and height), and the mean downstream current is 0.1 $m\,s^{-1}$. The data run begins prior to arrival of the first sediment-laden block at the downstream instrument position, and it continues until some time after the clear-water blocks from upstream pass the sensor. Depending on what kind of an averaging procedure (if any) is invoked to analyze the resultant SSC time series measured by the fixed sensor, Method 1 may produce erosion estimates that range from an instantaneous maximum of 5 units (at t_2) to a mean of 3 units (average from t_1 to t_4) or smaller (average from t_0 to beyond t_8). The averaging interval has evident implications for the magnitude of erosion estimates derived from Method 1, and this critical issue is discussed in detail later. For now, it is sufficient to note that an instantaneous SSC maximum would not, in general, be representative of the average erosion rate across the entire terrace. The very fact that there is along-stream variability in SSC indicates that other points along the terrace experienced less erosion than the instantaneous maximum might suggest. The methodological challenge for Method 1 is to find an averaging procedure that yields a representative erosion rate for the entire terrace surface.

Whereas Method 1 produces an instantaneous maximum erosion depth of 5 units in the example above, Method 2 yields a maximum value of only 3.3 units at t_3 (column 7, Table 2). Inherent to Method 2 is an expanding-block averaging procedure that, unlike Method 1, requires no explicit decisions about averaging interval length. Initial erosion estimates in Method 2 are very sensitive to the magnitude of SSC values in the first several time steps of integration, but a ''true'' average erosion estimate $[ED(T)=(1+5+4+2)/4=3$ units] for the eroded portion of the terrace is eventually attained at $T=t_4$. Thus, the two methods converge on the same result if appropriate averaging and integra-

Table 2. Example Erosion Depth Estimates using Method 2

Time	C_m	U	$\overline{U(T)}\cdot T$	$C_m\cdot U$	$\Sigma C_m\cdot U$	$ED(T)$	C_m	U	$\overline{U(T)}\cdot T$	$C_m\cdot U$	$\Sigma C_m\cdot U$	$ED(T)$
	(a) Unidirectional Flow						(b) Bidirectional Flow					
t_0	0	0.1	—	—	—	—	0	−0.1	—	0	—	—
t_1	1	0.1	0.1	0.1	0.1	1	5	0.3	0.3	1.5	1.5	5
t_2	5	0.1	0.2	0.5	0.6	3	1	−0.1	0.2	−0.1	1.4	7
t_3	4	0.1	0.3	0.4	1.0	3.3	2	0.3	0.5	0.6	2	4
t_4	2	0.1	0.4	0.2	1.2	3	4	−0.1	0.4	−0.4	1.6	4
t_5	0	0.1	0.5	0	1.2	2.4	0	0.3	0.7	0	1.6	2.3
t_6	0	0.1	0.6	0	1.2	0	−0.1	0.6	0	1.6	2.7	2
t_7	0	0.1	0.7	0	1.2	1.7	0	0.3	0.9	0	1.6	1.8
t_8	0	0.1	0.8	0	1.2	1.5	0	−0.1	0.8	0	1.6	2

tion intervals are chosen. Unfortunately, the appropriate averaging intervals are not known a priori or post facto under real circumstances, and there will always be methodological uncertainty regarding the ''true'' erosion rate.

In the scenario presented above, only steady unidirectional currents were considered. If this assumption is relaxed and an oscillatory component (ranging between -0.2 and 0.2 m s^{-1} with a 2 s period) is superposed on a downstream current of 0.1 m s^{-1}, then a new velocity time series ranging between -0.1 and 0.3 m s^{-1} is created (column 9, Table 2). Even given the same initial along-stream SSC distribution (column 8, Table 2), the new SSC time series measured by the fixed sensor under this oscillatory scenario would differ considerably from the unidirectional case, because the SSC boxes are advected past the OBS in a to-and-fro motion by the waves. Table 2 (column 13) shows the new erosion estimates from Method 2 based on this more complex example. The results are unstable, producing an unrealistic maximum erosion rate of 7 units at t_2. This instability was investigated in great detail using more complex SSC time series and by adopting different phase relationships with similarly peculiar outcomes. Cumulative sediment volume flux (proportional to $\Sigma C_m\cdot U$) and upstream contributing area [proportional to $\overline{U(T)}\cdot T$] were always predicted accurately as independent quantities, but the ratio leading toward $ED(T)$ was often not well behaved mathematically, because the denominator was sometimes very small (cumulative sum of positive and negative values) and $ED(T)$ therefore tended to infinity. In order to surmount this analytical quirk in Method 2, the absolute value of the velocity time series was used, and this is rationalized as follows.

Consider a single, isolated suspension plume with a horizontal width of 2 m and a uniform sediment concentration (SSC $=1$ unit). The plume is surrounded entirely by clear water. The positive thrust (crest) of a two-second wave moves the plume past a fixed sensor at an average velocity of 1 m s^{-1} for a time increment of one second. The sensor registers this positive sediment flux during time increment $T=t_0-t_1$, and Eqs. (1)–(4) provide estimates of $CA(t_1)$ equal to 1 m and of $ED(t_1)$ equal to one unit of erosion. If the wave period is twice as long, then the duration of the wave crest is $t_1=2$ s, and the sediment flux moving past the sensor during the new time increment increases twofold. Note that the estimate of $CA(t_1)$ also doubles; therefore, the estimate of $ED(t_1)$ remains the same (one unit of erosion). Now, reconsider the two-second wave with a positive thrust lasting one second, immediately followed by a negative thrust (wave trough) lasting one second. The original form of Eqs. (1)–(4) would have the positive sediment flux (associated with the wave crest) negated by the negative flux (associated with the wave trough), yielding a cumulative (net) sediment flux of zero at t_2. This would imply zero erosion in the system, which was clearly not the case given the existence of the sediment plume in the first instance. In addition, $CA(t_1-t_2)=-CA(t_0-t_1)$ such that the cumulative size of the contributing area at the end of the wave cycle also approaches zero $[CA(T)\Rightarrow 0]$. This leads to an unstable estimate for $ED(t)$, because the ratio approaches 0/0 as $t\Rightarrow t_2$. However, if the absolute value of the velocity is used, the result is the same as if the positive thrust of the wave had a duration of 2 s—that is, a doubling of sediment flux and a doubling of contributing area—yielding the correct estimate for $ED(t_2)$ of one erosion unit. Applying the absolute-value modification to the example in Table 2 produces a maximum erosion estimate of 5 units at t_1, with progressively decreasing values at longer times, and an anticipated ''true'' erosion estimate of 3 units between t_4 and t_5. This absolute-value approach provided well-behaved solutions under all scenarios investigated, and it was therefore adopted in the remainder of the paper. The conditions for which it is valid and appropriate are outlined in the Discussion section.

Results

Direct Bank Erosion Measurements

Although direct measurement of erosion rates due to individual boat wakes is currently not feasible, measurement of cumulative bank retreat over long periods is easily accomplished using crude technologies such as erosion pins. As part of a broader research agenda, a multiple boat-pass experiment was conducted involving 500 boat passages in rapid succession (i.e., over a period of a few hours on July 10, 1999). The same boat was driven back and forth past the field site at medium speed to maximize the wake waves ($H_{\max}\approx 0.25$ m) and to maintain semicontinuous wave forcing on the banks. At the conclusion of the experiment, cumulative erosion on the subaqueous terrace amounted to about 15 mm, which translates to an erosion rate of about 0.03 mm/boat passage. A similar experiment involving 1,000 boat passages was conducted on October 21–22, 2000, with average erosion rates of about 0.01–0.03 mm/boat passage. These direct measurements provide a robust standard against which the proposed algorithms can be evaluated.

Boat-Generated Waves

General hydrodynamic conditions associated with the seven midchannel boat passages are summarized in Table 1. Index wave height, H_i, was calculated using linear theory with a shallow-water approximation, $H_i=2U_m/\sqrt{(g/h)}$, where $g=$ gravitational

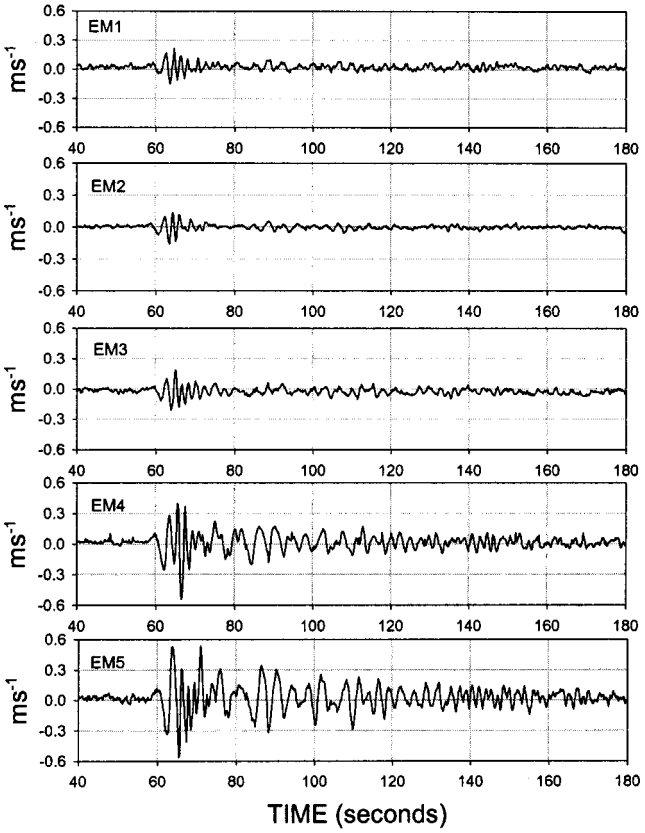

Fig. 5. Cross-shore velocity time series for Run 3

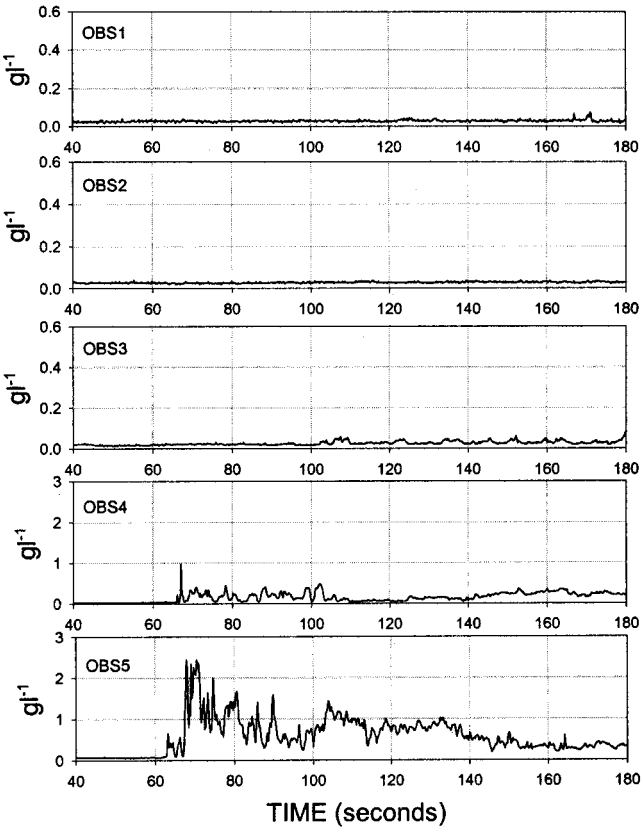

Fig. 6. Suspended sediment concentration time series for Run 3

acceleration, h = local water depth, and U_m = maximum near-bottom orbital velocity corresponding to the maximum onshore phase of waves measured at EM5 during each boat-wake event. For the boat used in this study, the largest waves were produced at speeds of about 12–15 knots. Wind-wave activity was negligible during the experiment, as seen in the initial segments of all velocity time series prior to arrival of a boat wake (Fig. 5). Boat-generated waves typically had a leading trough, and the first three wave crests were distinct and easily identifiable in the time series of EM1, EM2, and EM3 of the array. Such was the case for every boat passage monitored, and these first three waves are referred to as the primary wave packet. The duration of this primary wave packet (elapsed time from the initial zero-crossing of the leading wave trough to the crest of the third wave) was subsequently used as a normalizing variable to transform time.

Close to shore, the primary wave packet became increasingly contaminated by waves reflected off the bank, but the interaction of incident and reflected waves at near-bank positions is an integral part of the overall dynamics leading to sediment entrainment and erosion on the terrace. Sediment is affected equally by wave energy directed onshore (incident waves) or offshore (reflected waves). After periods of less than five minutes, hydrodynamic conditions were restored to background levels. Although it might appear from Fig. 5 that wave orbital velocities and resonances were more energetic and longer lasting at near-bank positions (e.g., at EM5), this is an artifact of instrument depth relative to the water surface. The outer current meters (EM1, EM2, and EM3) were located at lower depths in the water column (see Fig. 2); therefore, they were within the depth-attenuated portions of wave ellipses. In contrast, EM4 and EM5 were located in shallow water and closer to the mean water surface, and were thus fully exposed to maximum surface orbital velocities and to the full effect of shallow-water wave transformations.

Sediment Suspension

Comparison of velocity (Fig. 5) and sediment concentration (Fig. 6) time series reveals that near-bank suspension processes (i.e., at OBS5 and OBS4) were closely coupled to the dynamics of the primary waves in the boat-wake event. The first 3–5 wave half-cycles (crests and troughs) entrained progressively more sediment, and maximum concentrations were typically achieved after the third wave crest of the primary wave packet. Thereafter, turbidity levels remained high for periods of 40–80 s and then decreased to background levels within three to five minutes. The OBS calibrations (performed in an enclosed tub) demonstrated that, in the absence of agitation, elapsed settling times in excess of 30 minutes were required for suspended sediment mixtures to achieve concentrations less than 0.5 g L^{-1}. This supports the conclusion that clear water from upstream quickly swept away locally entrained sediments off the terrace.

Time series of suspended sediment concentration at offshore locations (i.e., OBS1, OBS2, and OBS3) show that turbidity rarely exceeded background levels in consequence of a boat passage (Fig. 6). This implies that either erosion was negligible (i.e., the water was too deep to be influenced by short surface waves) or these outer instruments were positioned too high in the water column to sense near-bottom suspension plumes. More importantly, the absence of a turbidity signal at these offshore instrument locations also suggests that very little sediment was dispersed from near-bank sources toward the center of the channel. Visual observations and photo/video recordings taken during the

experiment are consistent with this interpretation and reaffirm the dominance of downstream advection over dispersive-diffusive mixing.

Erosion Rate Estimates

The time series of velocity and sediment suspension discussed above imply that (1) boat-wake events strip layers of sediment from the bank and terrace; (2) mean currents advect the suspension plumes downstream or offshore; and (3) an eroded surface devoid of a depositional veneer is left behind. These conditions support the application of the two analytical methods developed in this study.

Method 1

Fig. 7 shows SSC time series measured at OBS5 for all seven boat-wake events. Each of the time series has had the time axis normalized by duration of the primary wave packet. Hereafter, all time axes are graduated in ''boat-packet increments'' rather than real time, and this facilitates comparison of different boat-wake events. These traces show that sediment was ''pumped'' into the water column during the primary wave packet (normalized times less than one) with several instantaneous peaks separated by low turbidity periods. Maximum prolonged turbidity levels were not typically attained until after the primary wave packet had passed, allowing sufficient time for mixing of hyperconcentrated suspension bubbles with surrounding water. Recall that Method 1 produces a time series of local bed-elevation change that has the exact same form as the SSC time series from which it was derived. An instantaneous maximum peak in the SSC time series, therefore, yields an instantaneous erosion rate that is very large—indeed, unrealistically large if taken as representative of the entire subaqueous terrace. In contrast, a long-term average taken over the entire time series (which may extend for tens of minutes and includes the gradual return to background turbidity levels) will produce erosion rates that are unrealistically small and functionally dependent on the length of the record rather than the local erosive effect of the boat-wake event. Therefore, an averaging algorithm is sought that can be applied in a consistent manner to produce robust estimates of erosion rate for only the most effective portion of the boat-wake event.

Fig. 8 shows the variation in means SSC with an averaging interval ranging from one through twelve ''boat-packet increments'' (excluding the ''pumping'' up period during the primary wave packet). The trends in Runs 3, 4, and 5 show initially large mean SSC followed by relatively rapid decay. Runs 1, 2, 6, and 7 are more complex, with mean SSC actually increasing toward a maximum as the averaging interval is extended over 2–4 normalized time increments (real times of approximately 20–40 s). This does not necessarily imply that more sediment was being entrained, but simply that prolonged wave agitation sustains large sediment concentrations in the water column for extended periods of time. In order to eliminate some of the arbitrary nature of selecting an appropriate averaging interval for Method 1, a series of linear regressions was performed to seek the best statistical correlation between mean SSC (as a function of averaging interval) and mean kinetic energy of the primary wave packet. Instantaneous near-bottom kinetic energy ($KE=\frac{1}{2}\rho[u^2+v^2]$ where ρ = fluid density and u,v = instantaneous cross-shore and alongstream velocity with background mean drift removed) was adopted as an index of the strength of waves to entrain sediments. Mean kinetic energy (averaged across the primary wave packet) was then used to parameterize the relative energetics of boat-wake events. The best-fit relationship between mean SSC and mean KE in the primary wave packet was produced when an averaging interval of five normalized time increments was used for SSC ($R^2=0.83$), but satisfactory results were also obtained using a SSC averaging interval of four normalized time increments or cumulative KE (rather than mean KE). This indicates that the overall erosion estimates appear to be somewhat insensitive to the exact averaging intervals chosen, although significantly longer or shorter averaging intervals yielded very poor regression results. Table 3 shows erosion estimates from Method 1 for Runs

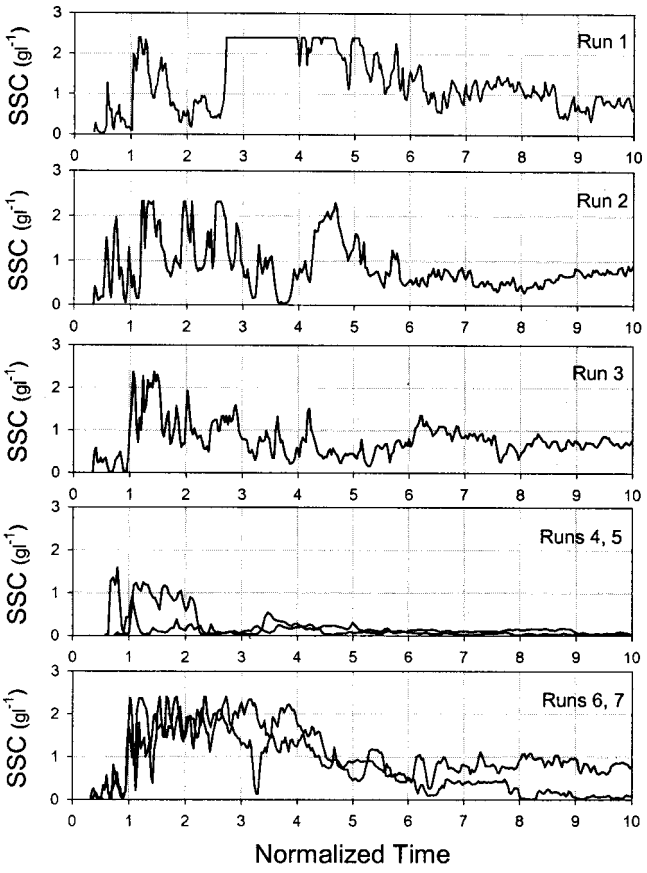

Fig. 7. Sediment suspension time series for all seven boat passages

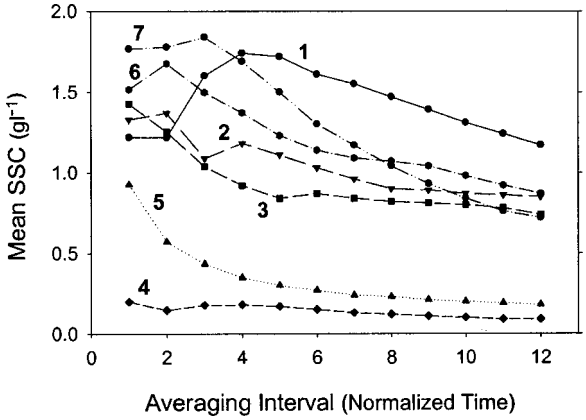

Fig. 8. Influence of averaging interval length on mean suspended sediment concentration for Runs 1–7; primary wave packet (normalized time between 0 and 1) excluded from these averages

Table 3. Erosion Estimates from Method 1

Run	Erosion (1–5)[a] (mm)	Erosion (1–6)[b] (mm)
1	0.223	0.220
2	0.135	0.127
3	0.098	0.089
4	0.018	0.016
5	0.030	0.026
6	0.107	0.096
7	0.113	0.100

[a]Method 1 erosion estimates using mean SSC averaged across normalized times of 1–5.

[b]Method 1 erosion estimates using mean SSC averaged across normalized time of 1–6.

1–7 using SSC averaging intervals of both four and five normalized time increments. The differences are trivial and within the range of experimental uncertainty.

Method 2

Sediment flux time series were generated by cross-multiplying comeasured time series of instantaneous horizontal velocity with suspended sediment concentration (e.g., Beach and Sternberg 1992; Aagaard and Greenwood 1994; Osborne and Vincent 1996). Cumulative sediment flux time series (i.e., the instantaneous series integrated across time) are particularly useful in providing insight into the dynamics of sediment transport, especially net transport direction. Fig. 9 shows both the instantaneous horizontal and cumulative sediment (mass) flux time series in the cross-shore and along-stream directions for Run 3. Mean preevent turbidity levels were removed from the original OBS time series, because these background signals are associated with bio-fouling and electronic noise in the instruments rather than sediment suspension. Preevent mean currents associated with the steady downstream flow of the river ($U_d \sim 0.02\ \mathrm{m\,s^{-1}}; V_d \sim 0.08\ \mathrm{m\,s^{-1}}$) were retained in the velocity records because they are important in determining net sediment drift directions. Time series of instantaneous sediment flux [Figs. 9(a and b)] show that little sediment transport occurred during the primary wave packet, especially in the along-stream direction. The bulk of sediment was moved during normalized times of one and two, and only isolated transport peaks occurred thereafter.

The cumulative sediment flux time series [Figs. 9(c and d)] show that sediment transport was generally directed onshore and downstream (positive values). The onshore trend in the cross-shore curve [Fig. 9(c)] suggests that the positive (onshore) phases of the boat-generated waves were more closely correlated with large sediment concentration plumes than were the negative (offshore) phases, thereby producing net sediment flux toward the bank. Maximum onshore values of cumulative flux were attained within only 4–6 normalized time increments, which indicates that net onshore transport ceased relatively early in the boat-wake event (within about 30 s). Such bank-directed fluxes ordinarily yield sediment accretion in the near-bank region, but this was not the case at the study site. Suspended sediments were flushed out of the system by downstream currents before they had time to settle, and net transport was persistently downstream despite weak onshore tendencies.

Fig. 10 shows time series of $ED(T)$ for Run 3 using Method 2 (with the absolute-value modification) for both the cross-shore and along-stream velocity time series. Cross-shore erosion estimates (maximum of 0.086 mm) are in accord with along-stream estimates (maximum of 0.097 mm), and this satisfying result was

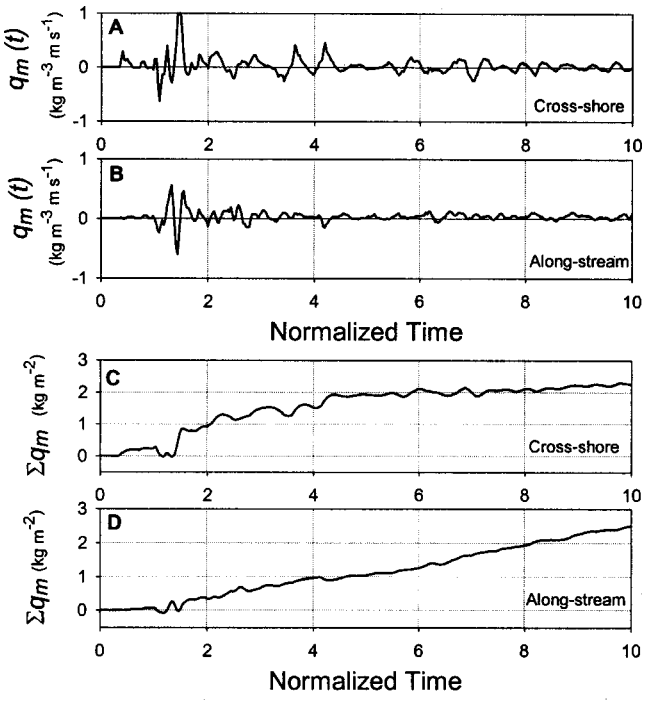

Fig. 9. Time series of sediment mass flux (q_m) and cumulative sediment mass transport (Σq_m) for Run 3 for both cross-shore (positive onshore) and along-stream (positive downstream) directions; background turbidity (SSC) prior to arrival of boat wake was subtracted from original OBS time series, but mean background currents were retained in original velocity time series.

common to all data runs, allowing a few generalizations to be drawn. $ED(T)$ is typically small during the primary wave packet, despite this being the most energetic portion of the boat-wake event when most sediment entrainment occurs. Relatively small amounts of sediment are transported past the OBS sensor during the primary wave packet (''pumping up'' period), and it is not until the secondary wave packet that large suspended sediment concentrations appear in the OBS traces (see Fig. 7). Fig. 10 shows that this is the period when $ED(T)$ rises sharply, after actual entrainment of sediment. Maximum erosion depth during Run 3 was approximately 0.09 mm (Fig. 10), and this occurred at normalized times between three and four. During other boat passages (e.g., Runs 1, 4, and 7), the time to maximum $ED(T)$ was delayed somewhat, but it never occurred later than a normalized time of six. Table 4 presents maximum $ED(T)$ estimates for all data runs using Method 2 (along-stream velocities only) and compares them with the averaged results from Method 1 (Table 3). Agreement between Method 1 and Method 2 estimates is excellent.

Discussion

Analytical methods such as those developed in this study are essential to evaluating the importance of recreational boat traffic to chronic levee erosion problems, because the actual (true) erosion rates per boat-wake event are too small to be measured directly using conventional surveying techniques. In the absence of direct bank erosion measurements, some uncertainty will always remain regarding the accuracy of erosion estimates based on indirect methods. Methods 1 and 2 converge on similar values of

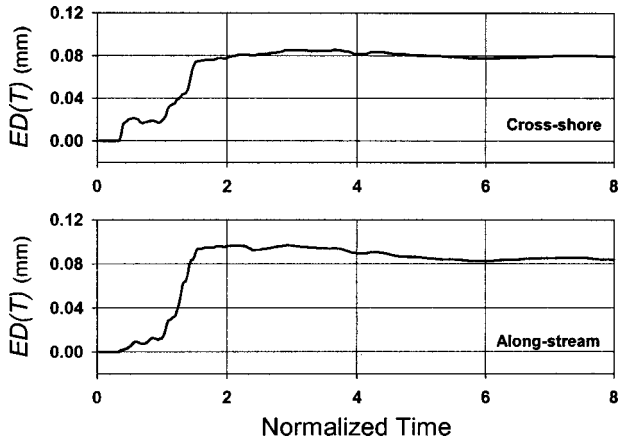

Fig. 10. Time series of erosion depth $[ED(T)]$ for Run 3 calculated using Method 2 with both cross-shore and along-stream velocity

erosion rate for each boat passage, thereby providing some assurance regarding the accuracy of the estimates. Unfortunately, these erosion estimates are 3–4 times greater on average than those obtained from the two multiple boat-passage experiments referred to earlier. There are many reasons why this might be so. First, the erosion estimates from the seven boat passages span a very large range (Table 4), and it is not known how representative the upper part of this range is of long-term bank erosion processes. Run 1 was clearly an unusual event in comparison with the others (Fig. 7), and eliminating it would greatly reduce the average erosion estimate. Second, there were obvious differences in the experimental conditions (e.g., tidal elevation, water temperature, algal coverings, bank-material strength, boat size) between the three sets of tests, which were conducted during different months of the year and over a span of several years. In this context, the erosion rates derived from each of the three experiments are not directly comparable. Third, there may be threshold erosion levels beyond which sediment stripping from the terrace is not as efficient as during the early stages of a multiple boat-passage experiment—that is, the first 10–50 (or more) boat passages might yield large erosion rates, whereas subsequent boat passages in the multiple boat sequence are less effective. These factors might explain why the average erosion rates obtained from the multiple boat-pass experiments were smaller than those from Methods 1 and 2. In either case, it is advantageous to understand the conditions for which the indirect methods are appropriately applied.

Table 4. Comparison of Method 1 and Method 2 Erosion Estimates

Run	Method 1[a] (mm)	Method 2[b] (mm)
1	0.222	0.193
2	0.131	0.135
3	0.094	0.097
4	0.017	0.015
5	0.028	0.051
6	0.101	0.100
7	0.106	0.093
Average	0.100	0.098

[a]Method 1 erosion estimates based on average values presented in Table 3.

[b]Method 2 erosion estimates based on absolute-value modification.

Some insight can be gained by substituting the integral equations [Eqs. (2) and (3)] into the expression for $ED(T)$ [Eq. (1)] and rearranging to get

$$ED(T)=\frac{A}{wp\rho_b}\frac{\frac{1}{T}\int_0^T C_m(t)\cdot U(t)dt}{\frac{1}{T}\int_0^T U(t)dt}=\frac{A}{wp\rho_b}\frac{\overline{C_m(t)\cdot U(t)}}{\overline{U(t)}} \tag{5}$$

where an overbar indicates a mean quantity averaged across the interval T. Employing a Reynolds decomposition scheme for the velocity $(U(t)=\overline{U}+U')$ and SSC $(C_m(t)=\overline{C}+C')$ time series, where a prime indicates a fluctuating component about the mean, and observing standard Reynolds' averaging rules leads to the following expression:

$$ED(T)=\frac{A}{wp\rho_b}\left[\overline{C}+\frac{\overline{C'U'}}{\overline{U}}\right] \tag{6}$$

This relationship shows that Method 2 and Method 1 converge only when the second term in the square brackets is small or zero (presuming the same averaging interval is used in Method 1 to obtain $\overline{C}$). The second term is a complex ratio that can assume any value within the domain of real numbers, and it is the source of difference between the two methods. The numerator in the second term is the covariance of the velocity and SSC time series, and it may assume positive or negative values (zero indicates no correlation and large values indicate close correlation). The denominator is the mean of the raw velocity time series, and it can assume positive or negative values, although with judicious choice of a reference frame it would ordinarily be positive.

Eq. (6) reveals the conditions for which the estimates from Method 1 and Method 2 are likely to converge, and also why Method 2 is occasionally unstable. During the initial phases of a boat-wake event, for example, oscillatory wave motion will dominate the velocity field and the short-term mean velocity $(\overline{U})$ will approach zero at specific times (sum of positive and negative phases). In addition, the field data show that there is a close coupling between the waves and sediment suspension, which suggests a high correlation (large covariance). Thus, the ratio $\overline{C'U'}/\overline{U}$ will be large, either positive or negative depending on whether the waves and sediments are positively or negatively correlated and on whether the short-term mean velocity is positive or negative. $ED(T)$ will be dominated by the second term and will deviate unrealistically from Method 1. In contrast, Method 2 will provide robust estimates of erosion when the absolute magnitude of the mean velocity (denominator) is large or if the SSC fluctuations are weakly correlated with the velocity fluctuations (i.e., $|\overline{U}|\gg\overline{C'U'}\approx 0$). Generally, such conditions are found in river environments where the downstream currents are strong and when sediment suspension is initiated by an impulse event with no preferred orientation to the wave motion, or by a boat passage with waves approaching the bank at a shore-perpendicular orientation. If the waves approach the bank at an oblique angle, there will be strong along-stream components in the velocity field, and these will likely be strongly correlated to sediment suspension. Similarly, Method 2 will not work well if bank erosion takes place in response to oblique wind-generated waves that are sustained for long periods of time or by tractive forces associated with strong flood flows.

The absolute-value modification to Method 2 is subject to similar constraints, and the reduced expression after Reynolds decomposition and averaging is

$$ED(T)=\frac{A}{wp\rho_b}\left[\overline{C}+\frac{\overline{C'|U(t)|}}{\overline{|U(t)|}}\right] \tag{7}$$

This expression is slightly more complex than Eq. (6) and it cannot be reduced without having additional information about the flow field. For example, if the velocity time series is always positive (i.e., $U(t)\geq 0$), then there is exact equivalence between Eqs. (6) and (7), making the absolute-value modification superfluous. In practice, this implies a strong downstream current or waves that produce only brief and small along-stream velocity reversals. More generally, the velocity time series might contain significant negative phases, as with large boat-generated waves oriented obliquely to the bank. Under such circumstances, it is not obvious how the ratio $\overline{C'|U(t)|}/\overline{|U(t)|}$ in Eq. (7) will compare to $\overline{C'U'}/\overline{U}$ in Eq. (6). Considering the denominators only, it is clear that $\overline{|U(t)|}\geq\overline{U}$, and also that $\overline{|U(t)|}\geq 0$. This demonstrates why the absolute-value ratio in Eq. (7) is better behaved than the unaltered ratio in Eq. (6).

The numerator of the absolute-value ratio in Eq. (7) is less intuitive, but using general rules that govern inequalities for averages and absolute values, it is easily shown that $\overline{C'|U(t)|}=\overline{C'|\overline{U}+U'|}\leq\overline{C'|\overline{U}|}+\overline{C'|U'|}=\overline{C'|U'|}$ and, in general, $|\overline{C'|U'|}|\leq|\overline{C'U'}|$. Together, these inequalities imply that $|\overline{C'|U(t)|}/\overline{|U(t)|}|\leq|\overline{C'U'}/\overline{U}|$, and this leads to the conclusion that the erosion estimate from the absolute-value modification of Method 2 [Eq. (7)] will deviate from the Method 1 estimate by a lesser amount (either positive or negative) than the unaltered velocity approach [Eq. (6)]. As before, the difference depends critically on the degree of phase coupling between the velocity and SSC fluctuations, and in general, it is advisable to restrict application of these methods to systems where such correlation is weak and where the mean along-stream velocity is large.

Although Method 1 is computationally less intensive and more intuitive, it is subject to the vagaries of arbitrarily selecting an appropriate averaging interval. There are few guidelines in the literature regarding this issue. Therefore, we recommend the use of Method 2 in conjunction with Method 1. Method 2 uses the information contained in both the velocity and SSC time series directly, and this more closely reflects the nature of sediment transport processes. Further, it does not require making decisions about representative averaging intervals—the erosion estimate [maximum value of the $ED(t)$ time series] is provided directly. Finally, in unsteady velocity fields, the correlation between SSC and the velocity pulses may be of great significance in assessing the transport and associated bottom erosion, and only Method 2 facilitates the inclusion of such pulses in the erosion estimate. If the estimates from Method 2 are significantly different than those from Method 1, the reasons for the divergence should be explored. On the other hand, if the results from both methods converge, then there is some assurance that a robust estimate of levee-bank erosion has been achieved.

Summary

A cross-shore array of electromagnetic current meters and optical back-scatterance sensors was deployed to measure the character of boat wakes and associated suspended sediment plumes. Boat-generated waves were readily distinguishable in velocity time series, and a primary wave packet was defined as the first three wave crests in a boat-wake event. In water depths of 0.5 m or less, suspended sediment plumes were in phase with the first three waves, indicating that orbital velocities were sufficient to erode sediment from the terrace bottom. Entrained sediments were swept away from the measurement site by the main channel flow. Boat wakes therefore entrain (rather than resuspend) new material and gradually erode levee banks.

Two alternative methods for estimating the magnitude of boat-wake-induced bank erosion were developed in this study. Method 1 uses only the OBS measurements and assesses erosion on the basis of a representative ''mean'' SSC during the boat-wake event. Method 1 is generally applicable to any system dominated by suspended sediment transport in which the horizontal gradients in sediment flux are small relative to the absolute magnitude of sediment flux. Velocity data are not incorporated into the algorithm, and it is therefore simple, but crude. Erosion estimates from Method 1 are very sensitive to the length (and centroid) of the chosen averaging interval. In this study, some of the arbitrariness of selecting a representative averaging interval was avoided by invoking a normalization scheme based on the duration of the primary wave packet. Intercomparisons among different boat runs were then possible to find an optimal averaging interval. Averaging intervals of 4–6 normalized time increments provided robust values for representative mean SSC. Longer intervals reduced the mean SSC (leading to minimal erosion estimates), whereas shorter intervals led to unstable estimates depending on the nature of the suspension plumes. In contrast, Method 2 incorporates both the OBS and current meter time series, as is conventional for nearshore sediment transport studies. These time series are cross-multiplied, and the resultant is integrated through time to yield the cumulative sediment volume transport. Division by the contributing (source) area from which the sediment is derived yields a time-dependent estimate for equivalent erosion depth. An absolute-value modification to Method 2 is recommended.

Time series of linear erosion show initial rapid stripping of sediment from the bed during the primary and secondary wave packets (i.e., approximately six complete wave cycles) followed by attainment of maximum erosion depths between normalized times of 2–4 (i.e., 6–12 waves). Erosion estimates from Method 1 and Method 2 are similar, and they range from less than 0.01 mm/boat passage for the weakest boat-wake event to 0.22 mm for the most energetic boat-wake event. The uppermost values are judged to overestimate the true erosion rate associated with single boat passages. Two multiple boat-passage experiments yielded erosion rates of roughly 0.01–0.03 mm/boat passage, which are in excellent agreement with the lower estimates from the analytical methods. These erosion rates are applicable only to this cohesive mud bank and the experimental techniques incorporated in the study—extrapolation to other sites and circumstances may be invalid except for purposes of determining general tendencies.

Acknowledgments

A large number of students are thanked for their assistance in the field, as are the editor (Zeki Demirbilek) and four anonymous reviewers for providing sound advice as well as astute and constructive criticism on earlier drafts. Steve Mello graciously allowed access to his land.

Notation

The following symbols are used in this paper:

A = cross-sectional area of plane perpendicular to flow;

$\overline{C}$ = short-term temporal mean sediment mass concentration;
C' = fluctuating component of sediment mass concentration;
$C_m(t)$ = instantaneous sediment mass concentration;
$CA(T)$ = contributing area from which sediment was derived;
$ED(T)$ = equivalent erosion depth;
g = gravitational acceleration;
H_i = index wave height;
h = water depth;
$Q_s(t)$ = instantaneous sediment volume discharge;
$Q_\Sigma(T)$ = cumulative sediment volume transport;
$q_m(t)$ = instantaneous sediment mass flux (mass discharge per unit area);
$q_s(t)$ = instantaneous specific sediment flux (volume discharge per unit area);
T = elapsed time since start of event;
t = time;
$\overline{U}$ = short-term temporal mean fluid velocity;
U' = fluctuating component of fluid velocity;
U_d = background mean cross-shore drift;
U_m = maximum near-bottom wave orbital velocity;
$U(t)$ = instantaneous fluid velocity;
u = instantaneous cross-shore velocity (background mean drift removed);
V_d = background mean along-stream drift;
v = instantaneous along-stream velocity (background mean drift removed);
wp = wetted perimeter;
ρ = fluid density; and
ρ_b = bulk density of in situ bottom sediment.

Subscripts

0,1,2 = specific values of time t.

References

Aagaard, T., and Greenwood, B. (1994). ''Suspended sediment transport and the role of infragravity waves in a barred surf zone.'' *Mar. Geol.*, 118, 23–48.

Anderson, F. E. (1974). ''The effect of boat waves on the sedimentary processes of a New England tidal flat.'' *Tech. Rep. No. 1*, Dept. of Earth Sciences, Univ. of New Hampshire, Durham, N.H.

Beach, R. A., and Sternberg, R. W. (1988). ''Suspended sediment transport in the surf zone: response to cross-shore infragravity waves.'' *Mar. Geol.*, 80, 61–79.

Beach, R. A., and Sternberg, R. W. (1991). ''Infragravity driven suspended sediment transport in the swash, inner and outer surf zone.'' *Proc., Coastal Sediments '91*, ASCE, New York, 114–128.

Beach, R. A., and Sternberg, R. W. (1992). ''Suspended sediment transport in the surf zone: response to incident wave and longshore current interaction.'' *Mar. Geol.*, 108, 275–294.

Bhowmik, N. G., and Demissie, M. (1983). ''Bank erosion by waves.'' *Proc. Frontiers in Hydraulic Engineering Conf.*, H. T. Shen, ed., ASCE, New York, 195–200.

Buckman, H. O., and Brady, N. C. (1969). *The nature and properties of soils*, 7th Ed., Macmillan, Toronto.

Camfield, F. E., Ray, R. E. L., and Eckert, J. W. (1980). ''The possible impact of vessel wakes on bank erosion.'' *Rep. No. CG-W-1-80*, U.S. Dept. of Transportation, Washington, D.C.

Collins, J. I., and Noda, E. K. (1971). ''Causes of levee damage in the Sacramento–San Joaquin Delta.'' *Internal Rep.*, Dept. of Navigation and Ocean Development, Sacramento, Calif.

Das, M. N., and Johnson, J. W. (1970). ''Waves generated by large ships and small boats.'' *Proc., 12th Engineering Conf.*, ASCE, New York, 3, 2281–2286.

Foda, M. A. (1995). ''Assessment of the erosion problem in the Sacramento–San Joaquin Delta: a critical review of previous studies.'' *Internal Rep.*, California Dept. of Boating and Waterways, Sacramento, Calif.

Garrad, P. N., and Hey, R. D. (1987). ''Boat traffic, sediment suspension, and turbidity in a Broadland river.'' *J. Hydrol.*, 95, 289–297.

Johnson, J. W. (1958). ''Ship waves in navigational channels.'' *Proc., 6th Conf. on Coastal Engineering*, ASCE, New York, 40, 666–690.

Johnson, J. W. (1968). ''Ship waves in shoaling waters.'' *Proc., 11th Int. Conf. on Coastal Engineering*, ASCE, New York, 96, 1488–1498.

Julien, P. Y. (1995). *Erosion and sedimentation*, Cambridge Univ. Press, New York.

Limerinos, J. T., and Smith, W. (1975). ''Evaluation of the causes of levee erosion in the Sacramento–San Joaquin Delta, California.'' *Water Resources Investigation 28–74*, U.S. Geological Survey, Menlo Park, Calif.

Madsen, O. S. (1991). ''Mechanics of cohesionless sediment transport in coastal waters.'' *Proc., Coastal Sediments '91*, ASCE, New York, 1, 15–27.

McLean, S. R. (1990). ''The stability of ripples and dunes.'' *Earth-Sci. Rev.*, 29, 131–144.

Nanson, G. C., von Krusentierna, A., Bryant, E. A., and Renilson, M. R. (1994). ''Experimental measurements of river-bank erosion caused by boat-generated waves on the Gordon River, Tasmania.'' *Regulated Rivers: Res. Manage.*, 9(1), 1–14.

Ofuya, A. O. (1970). ''Shore erosion—ship and wind waves, St. Clair, Detroit, and St. Lawrence Rivers.'' *Rep. No. 21, 14th Meeting of the Shore Erosion Committee*, Dept. of Public Works of Canada Design Branch Ontario.

Osborne, P. D., and Boak, E. H. (1999). ''Sediment suspension and morphological response under vessel-generated wave groups: Torpedo Bay, Auckland, New Zealand.'' *J. Coastal Res.*, 15(2), 388–398.

Osborne, P. D., and Vincent, C. E. (1996). ''Vertical and horizontal structure in suspended sand concentrations and wave-induced fluxes over bedforms.'' *Mar. Geol.*, 131, 195–208.